Construction of shell-model interactions for $Z \gtrsim 50$, $N \gtrsim 82$ nuclei: Predictions for $A = 133$–134 β^- decays

W.-T. Chou
Brookhaven National Laboratory, Upton, New York 11973
and Clark University, Worcester, Massachusetts 01610

E. K. Warburton
Brookhaven National Laboratory, Upton, New York 11973
(Received 13 September 1991)

Two shell-model interactions are constructed in the model space of the five proton and six neutron orbits just above the double shell closure at ^{132}Sn. One interaction uses the two-body matrix elements calculated by Kuo and Herling for use near ^{208}Pb. For the other, the proton-proton two-body matrix elements are replaced with effective ones of Kruse and Wildenthal and selected proton-neutron matrix elements were varied in order to better reproduce the known energy spectra of ^{134}Sb. The main difficulty in this construction is the determination of the neutron single-particle energies. This determination was done by comparison of theoretical and experimental (d,p) spectroscopic factors for the $N = 83$, $Z = 54$, 56, and 58 isotones. The $\Delta J \neq 0$ first-forbidden β^- decays of ^{133}Sn($\frac{7}{2}^-$), ^{134}Sn(0^+), ^{134}Sb(0^-), and ^{134}Sb(7^-) were considered in order to exemplify the application of these interactions.

PACS number(s): 23.40.Hc, 21.60.Cs, 23.40.Bw, 27.60.+j

I. INTRODUCTION

Recent advances in the spectroscopy of exotic nuclei have led to experimental information for numerous areas in the periodic table which were previously unstudied and even considered inaccessible. Of particular interest is the many attempts to approach and study magic and semi-magic domains. Examples of such domains are $Z,N = 28,50$; $Z,N = 40,40$; $Z,N = 50,50$; and $Z,N = 50,82$. Our interest in the last of these areas — in particular, the nuclei consisting of a few valance nucleons near doubly-closed ^{132}Sn — was aroused by the discovery of fast $\Delta J = 0$ first-forbidden β^- branches in the decays of ^{133}Sn, ^{134}Sn, and ^{134}Sb [1]. These decays offer the opportunity to extend the recent study [2] of such decays in the ^{208}Pb area to the next lower available doubly-magic domain.

We shall describe the construction of two shell-model interactions designed for the study of these decays. To date, β^- decay is the only process available for testing our interactions in these $A = 133$–134 nuclei. In this article we consider the $\Delta J \neq 0$ first-forbidden β^- decays of Table I. Our aim is to establish the viability of the interactions as well as possible with these rather

TABLE I. Fast first-forbidden β^- transitions in $A = 133$–134 nuclei. For the last six columns the number in parenthesis is the uncertainty in the least significant figure. For f_0, the number in square brackets is the power of ten. The data are from Refs. [1, 4–9]. When combining disparate values of Q_β and $T_{1/2}$, the resulting uncertainty was increased so that χ^2(per-degrees-of-freedom) was unity. In some cases uncertainties were not given in the literature. In those cases we have estimated them. The branching ratio is denoted by B.

Transition Initial	Transition Final	E_x (keV)	$T_{1/2}$ (sec)	Q_β (keV)	f_0	B (%)	$\log f_0 t$
^{133}Sn($\frac{7}{2}^-$)	^{133}Sb($\frac{7}{2}^+$)	0	1.35(12)[a]	7950(90)[b]	1.60(8)[+5]	85.0(50)	5.406(51)
^{133}Sn($\frac{7}{2}^-$)	^{133}Sb($\frac{5}{2}^+$)	962		6988(90)	9.0(5)[+5]	12.2(24)	6.005(98)
^{133}Sn($\frac{7}{2}^-$)	^{133}Sb($\frac{3}{2}^+$)	2708		5242(90)	5.84(7)[+2]	0.11(3)	7.49(13)
^{134}Sn(0^+)	^{134}Sb(0^-)	0	1.20(10)	7000(300)	9.07(17)[+4]	70.0(230)	5.192(17)
^{134}Sn(0^+)	^{134}Sb(1^-)	318		6682(300)	7.4(15)[+4]	1.4(7)	6.80(24)
^{134}Sn(0^+)	^{134}Sb(1^-)	872		6128(300)	5.0(11)[+4]	8.0(30)	5.88(19)
^{134}Sb(0^-)	^{134}Te(0^+)	0	0.75(7)	8410(160)	2.13(18)[+5]	97.5(25)	5.214(56)
^{134}Sb(0^-)	^{134}Te(2^+)	1279		7131(160)	1.02(11)[+5]	<0.5	>7.18
^{134}Sb(0^-)	^{134}Te(2^+)	2464		5946(160)	4.54(54)[+5]	0.2(1)	7.23(23)
^{134}Sb(0^-)	^{134}Te(1^+)	2632		5779(160)	4.00(49)[+5]	2.0(2)	6.177(80)
^{134}Sb(0^-)	^{134}Te(2^+)	2934		5476(160)	3.16(41)[+5]	0.3(2)	6.90(30)
^{134}Sb(7^-)	^{134}Te(6^+)	1691	10.43(14)	6813(150)	8.31(81)[+4]	43.0(30)	6.304(53)
^{134}Sb(7^-)	^{134}Te(6^+)	2398		6106(150)	5.11(56)[+4]	57.0(30)	5.971(53)

[a] Weighted average of 1.44 ± 0.04 s [4] and 1.20 ± 0.05 s [7].

[b] Weighted average of 7830 ± 70 keV [8] and 8013 ± 50 keV [6].

well understood observables before undertaking the more complex [2] $\Delta J = 0$ decays of Table I.

The formalism of first-forbidden β^- decay is complex and an adequate description of the procedures used to compare experimental and theoretical first-forbidden β^- decay rates is necessarily lengthy and involved. Such a description is given in the study [2] of the ^{208}Pb region and it would be inefficient and repetitious to present that description here. Rather, this present report is not intended to stand alone, but relies on the previous report [2] for an adequate description of the β^- processes. An important ingredient of the calculations is the calculation of the corrections due to core polarization. For an adequate description of these core polariztion corrections we rely on a recent treatment of the ^{208}Pb region [3] which was made to provide results for use in Ref. [2].

II. THE INTERACTIONS

The desired model space for the calculation of first-forbidden β^- decay observables in the $A = 134$ region includes, at the least, the five proton orbits and six neutron orbits between the doubly-closed shells at ^{132}Sn and ^{208}Pb. This model space — designated KH5082 — is shown schematically in Fig. 1. With a major oscillator shell designated by $Q = 2N + l$ [with N the principal quantum number (= 0,1,...) and l the orbital angular momentum], the five proton orbits are the $Q = 4$ major shell with the highest j orbit ($0g_{9/2}$) omitted and the highest j orbit of $Q = 5$ (the so-called "unique-parity" orbit) added. For the neutron orbits the situation is similar but with Q incremented by one unit. For brevity we designate these groups of orbits by primes, i.e., the proton and neutron model spaces are the $Q' = 4$ and 5 major shells, respectively.

The KH5082 interaction utilizes the two-body matrix elements (TBME) of the "bare + one-particle–one-hole (1p1h) bubble" Kuo-Herling (KH) interaction [10–12]. Two changes were made in these TBME. First, a glaring deficiency in the Kuo-Herling interaction is that the neutron-neutron $J = 0$ TBME are too attractive [11, 12]; thus, an approximate adjustment for this defect was made by multiplying these six TBME by 0.6. Second, the expected mass dependence of the residual interaction was taken into account by scaling all 2101 TBME by $(132/208)^{-1/3}$. The single-particle energies were taken from experiment. For the proton orbits the yrast states [4] were assumed to be the single-particle states thus giving the energies designated KH in Fig. 1. The yrast $J^\pi = \frac{1}{2}^+$ level is not known experimentally [4]; the excitation energy given in Fig. 1 was estimated from local systematics. The determination of the neutron single-particle energies is not as straightforward since the only levels reported in the literature are the ground state [4] and possibly a level at 1485 keV [13]. We assume the ground state to have $J^\pi = \frac{7}{2}^-$ and to be a single-particle $\nu 1f_{7/2}$ level. We follow Fogelberg *et al.* [1] in the identification of the 1485-keV level with the neutron $0h_{9/2}$ single-particle state. The other neutron single-particle energies of Fig. 1 were arrived at by comparison of theoretical and experimental energy centroids for the $Z = 54, 56$, and 58, $N = 83$ isotones. Because of dimensional restrictions, the proton model space in these calculations was confined to $\pi(0g_{7/2}, 1d_{5/2})^n$ with $n = 4, 6, 8$ and with at most two protons in the $1d_{5/2}$ orbit. The proton interaction of Kruse and Wildenthal [14] was used in this calculation (see below). The results for ^{141}Ce are shown in Fig. 2 in order to illustrate the approach. The experimental energy centroids $\langle E_j \rangle$ were evaluated from available (d, p) spectroscopic factors $S_n^+(j)$. The $S_n^+(j)$ for ^{141}Ce are from ^{140}Ce$(d, p)^{141}$Ce results of Park, Daehnick, and Spisak [15]. The shell-model values of $\langle E_j \rangle$ were obtained from calculations which included all states of a given j which had non-negligible spectroscopic strength. The sum of $S_n^+(j)$ over all experimental levels of a given j is less than unity for all j, i.e., there is missing spectroscopic strength. As shown in Fig. 2, there are many more levels expected than observed. Thus the missing strength is (at least partially) spread over many levels for which the $S_n^+(j)$ are below the threshold of perception. Since weak states become harder to observe as the excitation energy increases, it is most probable that the single-particle energies err some-

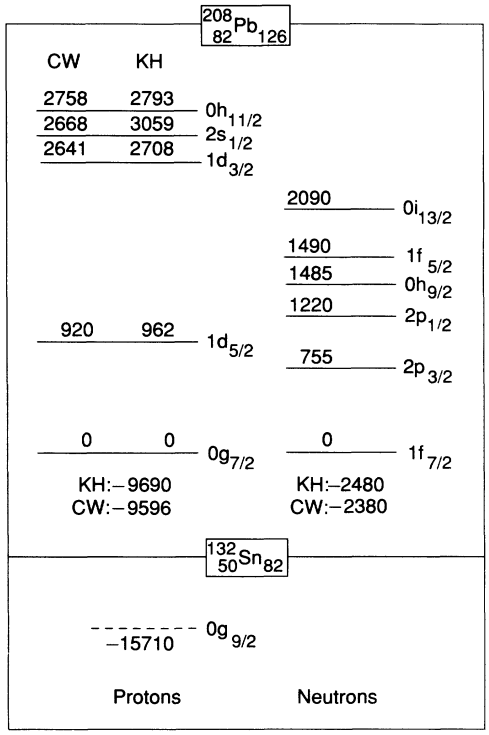

FIG. 1. Orbits contributing to the KH5082, CW5082, KH4082, and CW4082 interactions. The model spaces for the two 5082 interactions are for a $Z = 50$, $N = 82$ core and include all orbits between ^{132}Sn and ^{208}Pb. The model space for the 4082 interactions include the $\pi 0g_{9/2}$ orbit as well. As discussed in the text, the KH and CW forms of the interactions use somewhat different single-particle energies. Those used are indicated for each interaction in keV. The binding energies (in keV) relative to ^{132}Sn are given for the lowest proton and neutron orbits, the other energies are relative to these.

what on the low side. The predicted and experimental energy centroids for the $\nu 0h_{9/2}$ orbit are seen to be in rather poor agreement, i.e., the assumption [1, 13] of single-particle energies of 1485 keV for this orbit is not in good agreement with the assumptions of Ref. [15] as to the placement of the $\nu 0h_{9/2}$ spectroscopic strength. One reason for our adoption of the 1485-keV value from Refs. [1, 13] was that there appears to be considerable uncertainty in the placement of this strength as can be seen by comparing the assumed J^π values of Refs. [15] and [16]. It is because of deficiencies in the experimental data of this sort and the necessity of truncating the model space in the calculation of the $S_n^+(j)$ that more than one $N = 83$ isotone was considered. The final results of Fig. 1 are averages for the $Z = 54, 56, 58$ nuclei with ^{141}Ce weighed strongly because of the semiclosure of the $\pi 0g_{7/2}$ shell at $Z = 58$..

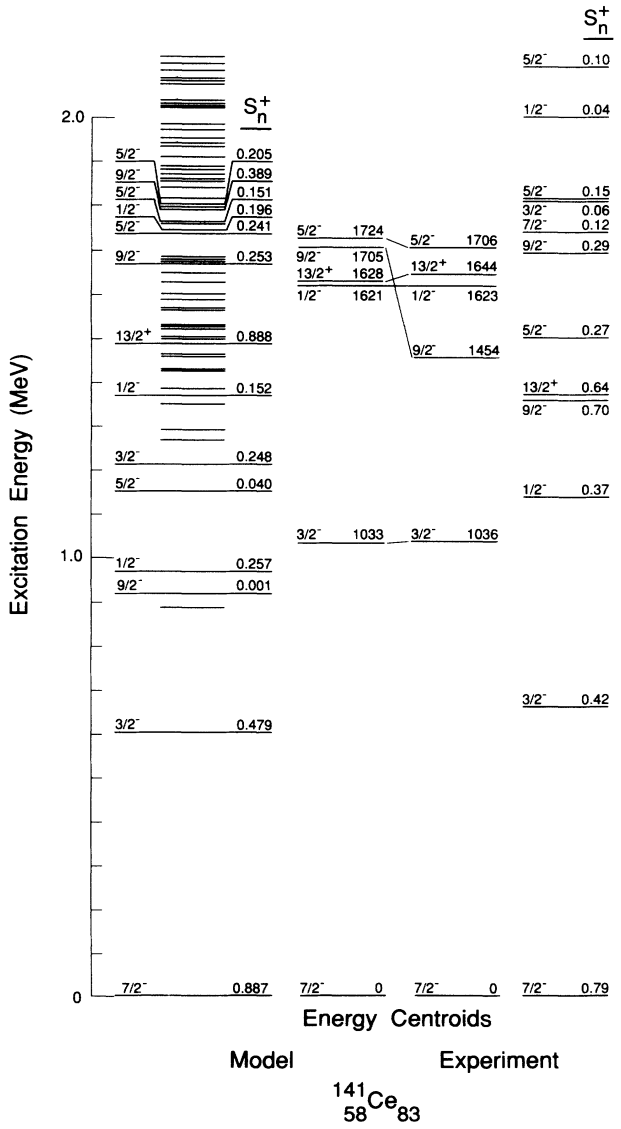

FIG. 2. Predicted and experimental energy spectra and energy centroids for ^{141}Ce. All levels reported in Ref. [15] below $E_x = 2.15$ MeV are shown. Predicted $S_n^+(j)$ are shown for the yrast $\pi(Q' = 4)$ orbits and for the level with the largest value of this stripping strength for each j. Other predicted levels below $E_x = 2.2$ MeV are indicated by lighter, shorter horizontal lines.

The KH5082 interaction is an attempt to build an interaction from fundamental principles. Another interaction — designated CW5082 — was constructed in order to better tune the interaction to local systematics. Thus, the CW5082 interaction was obtained from the KH5082 interaction by replacing the proton $Q' = 4$ TBME with the effective interaction of Kruse and Wildenthal [14] which is derived from a least-squares fit to binding energies with a surface-delta interaction as a starting point. The single-particle energies resulting from their least-squares fit were also adopted as shown in Fig. 1. In addition, the binding energies of the neutron orbits were decreased by 100 keV (see Fig. 1) and five proton-neutron TBME were modified as shown in Table II in order to reproduce the known $J = 0$ and 1 levels of ^{134}Sb [1].

The $\pi 0g_{9/2}$ orbit has a potentially strong role in first-forbidden β^- decay. Thus the $Z = 50, N = 82$ model spaces were expanded to include the $\pi 0g_{9/2}$ orbit. The 1043 TBME giving the interaction of the $\pi 0g_{9/2}$ orbit with itself and the $\pi Q' = 4$ and $\nu Q' = 5$ orbits were generated with the bare G-matrix potential (H7B) of Hosaka, Kubo, and Toki [17] together with the Coulomb potential. The $\pi 0g_{9/2}$ single-particle energy was set from the binding energy difference of ^{131}In and ^{132}Sn (see Fig. 1). Aside from the addition of the $\pi 0g_{9/2}$ orbit, the two model spaces with a $Z = 40, N = 82$ core are identical to the KH5082 and CW5082 model spaces and will be designated as KH4082 and CW4082, respectively. All calculations performed in the model spaces with a $Z = 40, N = 82$ core are done allowing simultaneously an inert (full) $\pi 0g_{9/2}$ orbit and a one particle-hole excitation out of this orbit together with full participation of the $\pi Q' = 4$ and $\nu Q' = 5$ shells.

In summary, two interactions were constructed in a conventional model space of the $\pi Q' = 4$, $\nu Q' = 5$ major shells. One interaction, KH5082, is based on a "bare G matrix + core polarization" calculation [10] and thus has characteristics reflecting our general knowledge of nuclear structure. The second interaction, CW5082, has a proton-proton part tuned to the energy levels of $Z > 50$ nuclei [14]. Two interactions are considered so that one can assess the sensitivity of predicted observables to the interaction by comparison of the two results. Finally,

TABLE II. The modifications made to four diagonal neutron-proton Kuo-Herling TBME to obtain better agreement with the ^{134}Sb experimental spectrum of Fig. 4 and to form the CW5082 and CW4082 interactions. The TBME are in MeV and Δ = KH − CW.

Orbits ij	J^π	$\langle ij\|V\|ij\rangle$ KH	CW	Δ
$0g_{7/2}1f_{7/2}$	0^-	−0.714	−0.678	−0.036
$0g_{7/2}1f_{7/2}$	1^-	−0.721	−0.336	−0.385
$1d_{5/2}1f_{7/2}$	1^-	−0.609	−0.326	−0.283
$0g_{7/2}0h_{9/2}$	1^-	−0.561	−0.279	−0.282
$0h_{11/2}0h_{9/2}$	1^+	−1.381	−1.187	−0.194

these two interactions are modified to the unconventional model space resulting from the addition of the $\pi 0g_{9/2}$ orbit. This is done because of a possibly large influence of this orbit on first-forbidden β^- observables similar to that found for the $\pi 0h_{11/2}$ orbit in the lead region.

III. CALCULATION

A. Energy spectra and scope of the study

Calculations were carried out with the computer code OXBASH [18]. The low-lying energy spectrum of ^{134}Sn calculated with the CW5082 interaction is shown in Fig. 3. The low-lying levels of ^{134}Sb calculated with the KH5082 and CW5082 interactions—both in a $\pi(Q'=4)\nu(Q'=5)$ model space—are compared to experiment in Fig. 4. Details of the ^{134}Sb energy spectrum and wave functions are given in Table III. The KH5082 and CW5082 spectra of ^{134}Te are compared to experiment in Fig. 5.

As detailed in Ref. [2], the β^- matrix elements are calculated via

$$M_R^\alpha = \sum_{j_i j_f} \mathcal{M}_R^\alpha(j_i j_f) = \sum_{j_i j_f} D_R(j_i j_f) M_R^\alpha(j_i j_f, \text{eff}) = \sum_{j_i j_f} D_R(j_i j_f) q_\alpha(j_i j_f) M_R^\alpha(j_i j_f). \quad (3.1)$$

In Eq. (3.1) α labels a particular type of matrix element which is of rank R, $M_R^\alpha(j_i j_f)$ is a single-particle matrix element for the transition $j_i \rightarrow j_f$ in the impulse approximation, and the renormalization factor $q_\alpha(j_i j_f)$ corrects $M_R^\alpha(j_i j_f)$ for the finite size of the model space. The $D_R(j_i j_f)$ are the one-body transition densities which are the result of the shell-model calculation performed with the code OXBASH [18].

We are interested in the prediction of β^- decay rates.

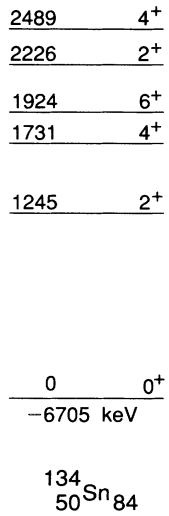

FIG. 3. The CW5082 predictions for the low-lying spectrum of ^{134}Sn. The predicted binding energy (relative to ^{132}Sn) is indicated beneath the ground state. There is no experimental information on this spectrum. The experimental binding energy to compare to the indicated predicted value is estimated to be -6560 ± 200 keV (see Sec. IV B).

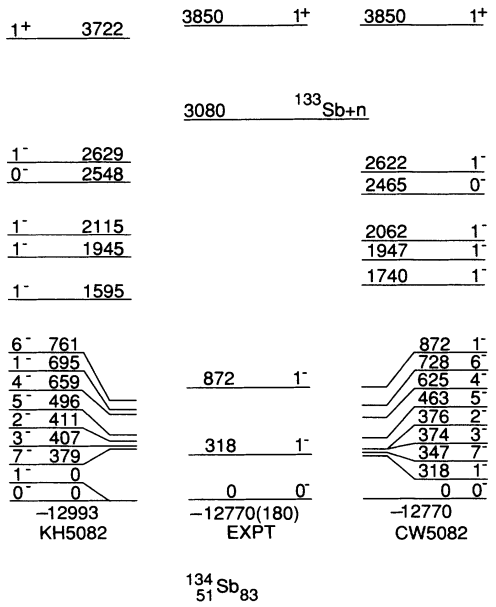

FIG. 4. Comparison to experiment of the KH5082 and CW5082 predictions for the low-lying spectrum of ^{134}Sb. All energies are in keV. Predicted and experimental binding energies (relative to ^{132}Sn) are indicated for the ground states. The only experimental known levels are shown. The nine lowest predicted levels are shown as well as all predicted $J=0$ and 1 levels below the experimental neutron binding energy of 3080 keV.

In any decay $J_i \rightarrow J_f$, matrix elements whose rank obeys

$$|J_i - J_f| \leq R \leq |J_i + J_f| \quad (3.2)$$

can contribute. The decay rate is incoherent in the rank R and comparison between experiment and theory can

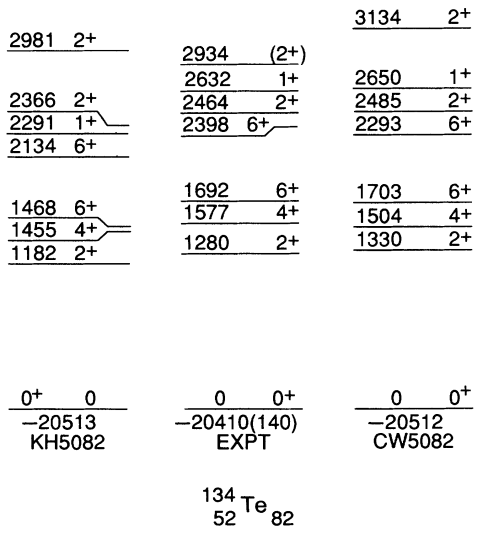

FIG. 5. Comparison to experiment of the KH5082 and CW5082 predictions for the low-lying spectrum of ^{134}Te. All energies are in keV. Predicted and experimental binding energies (relative to ^{132}Sn) are indicated for the ground states. The experimental levels are from Ref. [1]. The seven lowest predicted levels and the $J_k^\pi = 2_3^-$ level are shown.

TABLE III. The CW5082 spectrum of ^{134}Sb. The index k orders the states of given J^π in energy. Only $k \leq 3$ levels are shown. Dominant configurational contributions to the wave functions are indicated.

E_x (keV)	J^π	k	Dominant configurations
−12768	0^-	1	95.5% $\pi g_{7/2}\nu f_{7/2}$
321	1^-	1	87.5% $\pi g_{7/2}\nu f_{7/2}$
347	7^-	1	99.4% $\pi g_{7/2}\nu f_{7/2}$
374	3^-	1	90.5% $\pi g_{7/2}\nu f_{7/2}$
376	2^-	1	85.7% $\pi g_{7/2}\nu f_{7/2}$
463	5^-	1	89.7% $\pi g_{7/2}\nu f_{7/2}$
625	4^-	1	90.9% $\pi g_{7/2}\nu f_{7/2}$
728	6^-	1	96.1% $\pi g_{7/2}\nu f_{7/2}$
871	1^-	2	64% $\pi d_{5/2}\nu f_{7/2}$ + 14% $\pi g_{7/2}\nu h_{9/2}$
881	2^-	2	39% $\pi d_{5/2}\nu f_{7/2}$ + 34% $\pi g_{7/2}\nu p_{3/2}$
1035	6^-	2	97.0% $\pi d_{5/2}\nu f_{7/2}$
1218	4^-	2	47% $\pi d_{5/2}\nu f_{7/2}$ + 22% $\pi g_{7/2}\nu p_{3/2}$
1234	2^-	3	46% $\pi g_{7/2}\nu p_{3/2}$ + 28% $\pi d_{5/2}\nu f_{7/2}$
1265	3^-	2	45% $\pi d_{5/2}\nu f_{7/2}$ + 34% $\pi g_{7/2}\nu p_{3/2}$
1317	5^-	2	76% $\pi g_{7/2}\nu p_{3/2}$ + 12% $\pi d_{5/2}\nu f_{7/2}$
1438	4^-	3	41% $\pi g_{7/2}\nu p_{3/2}$ + 25% $\pi d_{5/2}\nu f_{7/2}$
1454	3^-	3	51% $\pi g_{7/2}\nu p_{3/2}$ + 40% $\pi d_{5/2}\nu f_{7/2}$
1549	5^-	3	84% $\pi d_{5/2}\nu f_{7/2}$ + 12% $\pi g_{7/2}\nu p_{3/2}$
1589	8^-	1	100% $\pi g_{7/2}\nu h_{9/2}$
1740	1^-	3	39% $\pi g_{7/2}\nu h_{9/2}$ + 19% $\pi d_{5/2}\nu f_{7/2}$
1745	3^+	1	95.7% $\pi h_{11/2}\nu h_{9/2}$
1746	6^-	3	79% $\pi g_{7/2}\nu f_{5/2}$ + 14% $\pi g_{7/2}\nu h_{9/2}$
2180	7^-	2	97.8% $\pi g_{7/2}\nu h_{9/2}$
2232	10^+	1	98.4% $\pi 9_{7/2}\nu i_{13/2}$
2365	4^+	1	90.3% $\pi g_{7/2}\nu i_{13/2}$
2465	0^-	2	81% $\pi d_{5/2}\nu f_{5/2}$ + 12% $\pi d_{3/2}\nu p_{3/2}$
2512	8^+	1	95.5% $\pi g_{7/2}\nu i_{13/2}$
2514	5^+	1	91.4% $\pi g_{7/2}\nu i_{13/2}$
2530	6^+	1	95.2% $\pi g_{7/2}\nu i_{13/2}$
2605	9^+	1	39% $\pi g_{7/2}\nu i_{13/2}$ + 37% $\pi h_{11/2}\nu f_{7/2}$
2680	7^+	1	88.3% $\pi g_{7/2}\nu i_{13/2}$
2885	7^-	3	97.2% $\pi d_{5/2}\nu h_{9/2}$
2940	9^+	2	57% $\pi g_{7/2}\nu i_{13/2}$ + 38% $\pi h_{11/2}\nu f_{7/2}$
2986	2^+	1	97.1% $\pi h_{11/2}\nu f_{7/2}$
3184	7^+	2	60% $\pi h_{11/2}\nu f_{7/2}$ + 17% $\pi h_{11/2}\nu p_{3/2}$
3274	4^+	2	57% $\pi h_{11/2}\nu f_{7/2}$ + 36% $\pi d_{5/2}\nu i_{13/2}$
3311	5^+	2	70% $\pi h_{11/2}\nu f_{7/2}$ + 8% $\pi h_{11/2}\nu p_{3/2}$
3312	3^+	2	91.2% $\pi h_{11/2}\nu f_{7/2}$
3403	6^+	2	77% $\pi h_{11/2}\nu f_{7/2}$ + 20% $\pi d_{5/2}\nu_{i13/2}$
3450	8^+	2	79% $\pi h_{11/2}\nu f_{7/2}$ + 20% $\pi d_{5/2}\nu_{i13/2}$
3566	9^+	3	72% $\pi d_{5/2}\nu i_{13/2}$ + 25% $\pi h_{11/2}\nu f_{7/2}$
3579	4^+	3	53% $\pi d_{5/2}\nu i_{13/2}$ + 32% $\pi h_{11/2}\nu f_{7/2}$
3710	5^+	3	78% $\pi d_{5/2}\nu i_{13/2}$ + 16% $\pi h_{11/2}\nu f_{7/2}$
3711	7^+	3	72% $\pi d_{5/2}\nu i_{13/2}$ + 23% $\pi h_{11/2}\nu f_{7/2}$
3789	0^-	3	70% $\pi d_{3/2}\nu p_{3/2}$ + 16% $\pi d_{5/2}\nu f_{5/2}$
3848	1^+	1	100% $\pi h_{11/2}\nu h_{9/2}$
3848	6^+	3	75% $\pi d_{5/2}\nu i_{13/2}$ + 19% $\pi h_{11/2}\nu f_{7/2}$
3898	8^+	3	79% $\pi d_{5/2}\nu i_{13/2}$ + 20% $\pi h_{11/2}\nu f_{7/2}$
4140	2^+	2	97.1% $\pi h_{11/2}\nu h_{9/2}$
4386	10^+	2	98.4% $\pi h_{11/2}\nu h_{9/2}$
4471	3^+	3	72% $\pi h_{11/2}\nu f_{5/2}$ + 21% $\pi h_{11/2}\nu h_{9/2}$
5536	9^-	1	100% $\pi h_{11/2}\nu i_{13/2}$
5554	10^-	1	100% $\pi h_{11/2}\nu i_{13/2}$
5664	8^-	2	100% $\pi h_{11/2}\nu i_{13/2}$

be conveniently formulated via the square root of the averaged shape factor $\langle C(W)\rangle^{1/2}$, where the experimental shape factor is defined by [2]

$$\langle C(W)\rangle = \frac{9195 \times 10^5}{f_0 t}\ \text{fm}^2. \tag{3.3}$$

In Eq. (3.3) W is the β^- decay energy and the shape factor modifies the "allowed" shape of the β spectrum extending from $W = 1$ to W_0, where W_0 is the total disintegration energy. The theoretical shape factor contains all the information on the nuclear matrix elements and is defined as the sum of the $R = 0$ ($R0$), $R = 1$ ($R1$), and $R = 2$ ($R2$) contributions (beta moments) [2].

$$\overline{C(W)} = B_1^{(0)} + B_1^{(1)} + \frac{1}{3}\overline{q^2 + \lambda_2 p^2} B_1^{(2)}\ , \tag{3.4}$$

where q and p are the neutrino and electron momenta and λ_2 is a Coulomb function. The $R2$ moment $B_1^{(2)}$ contains only one matrix element, M_1^z, which is the $R2$ member of the (schematic) operator $[\mathbf{r}, \boldsymbol{\sigma}]^R$. The $R1$ moment $B_1^{(1)}$ is a combination of the $R1$ member of this operator, M_1^u, and of the exact analogue of the $E1$ operator, M_1^x. The shape factor can be formulated as

$$C(W) = k(1 + aW + b/W + cW^2). \tag{3.5}$$

To illustrate how one combines the two $R1$ matrix elements to obtain $B_1^{(1)}$, the leading (energy independent) term of Eq. (3.5) is expressable as

$$k = [a_u M_1^u - a_x M_1^x]^2 \tag{3.6}$$

where the a_α are positive kinematical factors — dependent on Z, W_0, and the nuclear radius — which can be accurately evaluated.

We shall consider those $R1$ and $R2$ first-forbidden β^- decays of ^{133}Sn($\frac{7}{2}^-$), ^{134}Sn(0^+), and the two known isomers of ^{134}Sb which are listed in Table I as well as some $R1$ and $R2$ transitions to higher states. The first-forbidden decay of ^{133}Sn to ^{133}Sb is shown schematically in Fig. 6. We are interested in the decay connecting the leading terms and in the core polarization terms connecting in first order to the leading terms. Because of Pauli blocking the only particle-hole (p-h) admixtures in the

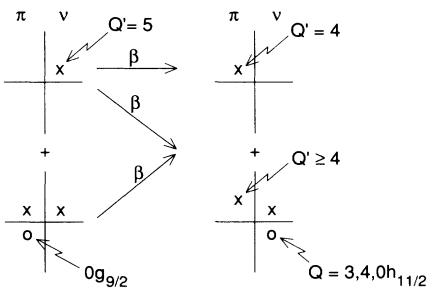

FIG. 6. Schematic illustrating the contributions included in the calculation of ^{133}Sn $\xrightarrow{\beta^-}$ ^{133}Sb β^- decay. The leading terms are at the top and an example of a 1p-1h admixture in the initial state (left) and a "final-state correlation" in the final state (right) are at the bottom.

initial state which connect to the leading term in the final state are those involving the $\pi 0g_{9/2}$ orbit and are included in the diagonalization. The radial integrals involved in the single-particle transitions were evaluated using Woods-Saxon (WS) radial wave functions as discussed in Ref. [2].

First-forbidden decays have the selection rule $\Delta Q = \pm 1$ governing the transitions between the initial and final orbits so that they must lie in adjacent major shells. The final-state correlations illustrated in Fig. 6 are reached from the leading term in the initial state via $\nu(Q = 3) \rightarrow \pi(Q = 4)$, $\nu(Q = 4) \rightarrow \pi(Q = 5)$, and $\nu 0h_{11/2} \rightarrow \pi(Q' = 4) + \pi(Q = 6)$ transitions. These terms are added perturbatively via the renormalization factors $q_\alpha(j_i j_f)$ [3] of Eq. (3.1).

Values of the $q_\alpha(j_i j_f)$ for the "closed core plus one" case of $^{133}\mathrm{Sn} \xrightarrow{\beta^-} {}^{133}\mathrm{Sb}$ are collected in Table IV for the five first-forbidden operators we use to describe these decays. These $q_\alpha(j_i j_f)$ were used for all decays considered. Two different residual interactions were used in these calculations. Both were derived from G-matrix potentials. That designated H7B is from Hosaka, Kubo, and Toki [17] and was used in the previous calculations in the lead region [3]. The H7B interaction is based on the Paris [19] nucleon-nucleon potential. Hosaka [20] has also made a fit with the same potential form to the Bonn [21] nucleon-nucleon G matrix. This interaction — designated HBB — was also considered because a comparison of the H7B and HBB results gives some idea of the dependence of the core polarization on the residual interaction used. In particular, the Bonn potential has a tensor component about 25% weaker than that of the Paris potential and, as fully discussed elsewhere, the dependence on the tensor contribution is of particular interest especially for the $R0$ beta moment not considered here [22, 3, 2, 23]. Harmonic oscillator (HO) radial wave functions were used in these calculations since it was found [3, 2] that the q_α are relatively insensitive to the form of the radial wave functions. We note that the results of Table IV bear a strong similarity to those calculated for $A = 209$–212 nuclei [3]. This similarity is expected since the $A = 133$–137 model space is derived from that for the $A = 209$–212 nuclei by lowering the Q' of the neutron and proton spaces by one unit. The number of p-h transitions contributing to the $q_\alpha(j_i j_f)$ are 10, 27, and 33 for $R0$, $R1$, and $R2$, respectively. It is seen that the summed intensity of these p-h terms in the final-state wave function is generally quite small so that a first-order perturbation treatment is well justified. There is one exception, namely, the contribution of the $\nu 0h_{11/2} \rightarrow \pi 0g_{7/2}$ "final-state correlation" to the $R2$ $\nu 1f_{7/2} \rightarrow \pi 1d_{3/2}$ transition. This contribution arises from a $\{[\nu 1f_{7/2}] \otimes [(\nu 0h_{11/2})^{-1} \pi 0g_{7/2}]_{2^-}\}_{3/2^+}$ admixture in the final state, which for the perturbative HBB calculation is 9.6% of the total p-h admixture of 10.8% and which contributes ~70% of the quenching of this transition. A major reason for the large contribution of this p-h term to the $\pi 1d_{3/2}$ state of ^{133}Sb is that this $\frac{3}{2}^+$ state is considerably further removed from the Fermi surface than the ^{133}Sb states involved in the other two $A = 133$ transitions considered here, namely, the

TABLE IV. Renormalization factors $q_\alpha(j_i j_f)$ calculated for $A \approx 132$ nuclei with HO wave functions and both the H7B and HBB residual interactions. Results are for the five M_R^α matrix elements ($\alpha = S, T, u, x$, and z) defined in Ref. [2]. The q_S are not listed since for HO wave functions, $1 - q_S = q_T - 1$. The total sum of the final state admixtures which contribute to the process for the HBB interaction is also given.

Transition	p-h (%)	H7B	HBB
		q_T	
$0h_{9/2} \rightarrow 0g_{9/2}$	0.47	1.1260	1.1347
$1f_{7/2} \rightarrow 0g_{7/2}$	0.17	0.8390	0.8927
$1f_{5/2} \rightarrow 1d_{5/2}$	0.36	1.1277	1.1401
$2p_{3/2} \rightarrow 1d_{3/2}$	0.23	0.9309	0.9698
$2p_{1/2} \rightarrow 2s_{1/2}$	0.20	1.0659	1.0859
		q_u	
$0h_{9/2} \rightarrow 0g_{9/2}$	2.03	0.5948	0.6111
$0h_{9/2} \rightarrow 0g_{7/2}$	3.39	0.3555	0.4016
$1f_{7/2} \rightarrow 0g_{9/2}$	0.42	0.6334	0.6519
$1f_{7/2} \rightarrow 0g_{7/2}$	0.74	0.5596	0.6030
$1f_{7/2} \rightarrow 1d_{5/2}$	2.03	0.4698	0.5071
$1f_{5/2} \rightarrow 0g_{7/2}$	0.46	0.6879	0.7236
$1f_{5/2} \rightarrow 1d_{5/2}$	1.71	0.5168	0.5462
$1f_{5/2} \rightarrow 1d_{3/2}$	1.81	0.3849	0.4307
$2p_{3/2} \rightarrow 1d_{5/2}$	0.52	0.5852	0.6183
$2p_{3/2} \rightarrow 1d_{3/2}$	0.53	0.5512	0.5987
$2p_{3/2} \rightarrow 2s_{1/2}$	0.62	0.5323	0.5746
$2p_{1/2} \rightarrow 1d_{3/2}$	0.28	0.6059	0.6482
$2p_{1/2} \rightarrow 2s_{1/2}$	0.71	0.5158	0.5553
$0i_{13/2} \rightarrow 0h_{11/2}$	4.25	0.4677	0.4910
		q_x	
$0h_{9/2} \rightarrow 0g_{9/2}$	2.03	0.5778	0.6172
$0h_{9/2} \rightarrow 0g_{7/2}$	3.39	0.6156	0.6751
$1f_{7/2} \rightarrow 0g_{9/2}$	0.42	0.7738	0.7874
$1f_{7/2} \rightarrow 0g_{7/2}$	0.74	1.0087	1.0819
$1f_{7/2} \rightarrow 1d_{5/2}$	2.03	0.6850	0.7368
$1f_{5/2} \rightarrow 0g_{7/2}$	0.46	0.7379	0.7740
$1f_{5/2} \rightarrow 1d_{5/2}$	1.71	0.5889	0.6331
$1f_{5/2} \rightarrow 1d_{3/2}$	1.81	0.6194	0.6756
$2p_{3/2} \rightarrow 1d_{5/2}$	0.52	0.7823	0.8139
$2p_{3/2} \rightarrow 1d_{3/2}$	0.53	0.8561	0.9094
$2p_{3/2} \rightarrow 2s_{1/2}$	0.62	0.7488	0.7998
$2p_{1/2} \rightarrow 1d_{3/2}$	0.28	0.7869	0.8297
$2p_{1/2} \rightarrow 2s_{1/2}$	0.71	0.7028	0.7482
$0i_{13/2} \rightarrow 0h_{11/2}$	4.25	1.2935	1.2536
		q_z	
$0h_{9/2} \rightarrow 0g_{9/2}$	0.67	0.6475	0.6560
$0h_{9/2} \rightarrow 0g_{7/2}$	1.31	0.3937	0.4333
$1f_{7/2} \rightarrow 0g_{9/2}$	0.17	0.8481	0.8500
$1f_{7/2} \rightarrow 0g_{7/2}$	0.16	0.7221	0.7009
$1f_{7/2} \rightarrow 1d_{5/2}$	2.03	0.4168	0.4454
$1f_{7/2} \rightarrow 1d_{3/2}$	10.77	0.1212	0.1654
$1f_{5/2} \rightarrow 0g_{9/2}$	0.17	0.8582	0.8549
$1f_{5/2} \rightarrow 0g_{7/2}$	0.17	0.8594	0.8765
$1f_{5/2} \rightarrow 1d_{5/2}$	0.82	0.4193	0.4435
$1f_{5/2} \rightarrow 1d_{3/2}$	0.33	0.4842	0.5304
$2p_{3/2} \rightarrow 1d_{5/2}$	0.28	0.7215	0.7342
$2p_{3/2} \rightarrow 1d_{3/2}$	0.23	0.4833	0.4876
$2p_{3/2} \rightarrow 2s_{1/2}$	1.60	0.4647	0.4919
$2p_{1/2} \rightarrow 1d_{5/2}$	0.34	0.6994	0.7104
$2p_{1/2} \rightarrow 1d_{3/2}$	0.14	1.0788	1.1358
$0i_{13/2} \rightarrow 0h_{11/2}$	3.48	0.4490	0.4629

$\pi 0g_{7/2}$ and $\pi 1d_{5/2}$ states (see Fig. 1). Because of this large contribution, a proper treatment of this particular transition demands an expansion of the model space to include neutron-hole states from below the $N = 82$ shell closure, i.e., a perturbative treatment of such a large contribution will certainly have a large uncertainty and the $\nu 2s_{1/2}$ and $\nu 1d_{3/2}$ orbits should probably be included as well as the $\nu 0h_{11/2}$ orbit even though they do not have a first-order effect on the first-forbidden β^- decays under consideration. Nevertheless, we present these results for this questionable $R2$ transition in this first attempt as a quantitative explanation of these decay rates.

IV. RESULTS AND DISCUSSION OF INDIVIDUAL DECAYS

Comparison of theory and experiment is made in Table V for the $\Delta J \neq 0$ decays of Table I. The results for the two interactions CW4082 and KH4082 are only marginally different as are the results using the two sets of q_α of Table IV. We will use the CW4082 result with the HBB core polarization in the following discussions. Before undertaking a description of individual decays, we consider some general features of the predictions vis-à-vis those found previously [2] in the lead region.

The $\Delta J = 1$ decays considered all have dominant $R1$ contributions; the $R2$ contribution is less than 10% in all cases. Nevertheless, the relative $R2/R1$ ratio has increased by a factor of over 10 from the lead region. The causes for this increase have to do with the relative kinematics. Firstly, the $R1$ contribution has terms proportional to Z while the $R2$ contribution does not. Secondly, in the lead region the $R1$ contribution is dominated by the allowed term with the result that the zeta approximation [2]—in which only the first term of Eq. (3.5) is retained—is a good representation. The transitions considered here in the tin region have $Z \approx 50$ rather than $Z \approx 82$, Q_β values 2–3 times larger, and Coulomb displacement energies of about the same magnitude. The result is a strong cancellation between the Coulomb and energy terms [see Eq. (28) of Ref. [2]] for the M_1^u matrix element which dominates the $R1$ process in the lead region while the other $R1$ matrix element, M_1^x, is somewhat enhanced at $A \sim 132$ and is now dominant. Another change is that the zeta approximation—which is quite accurate in the lead region—is not even approximately correct. That is, in the tin region it is imperative that the full $R1$ shape factor of Eq. (3.5) be considered rather than just the first term.

A general and important feature of the $R1$ decays of Table V is that the two matrix elements M_1^u and M_1^x in terms of which the $R1$ decay rate is formulated [2] have the same sign. A result of this is that their contributions add destructively in all four terms of the shape factor. This is illustrated in Eq. (3.6) for the energy independent term of the shape factor [Eq. (3.5)]. Thus the $R1$ decay rates are noticeably more sensitive to details of the nuclear structure than if they combined constructively. In view of this sensitivity, the overall agreement of the comparison of Table V can be termed satisfactory. Since similar orbits — albeit one major shell away — are involved as in decays in $A = 209$ and 210 nuclei [2], it is not surprising that the relationship between the $R1$ matrix elements are quite similar in the two regions. Thus the discussion of this relationship given in Ref. [2] is pertinent here also.

For purposes of the following discussion, the decays of Table V can be divided into two groups. One for which the final-state wave function is relatively pure and the other for which the final-state wave function is mixed. The first group includes the two ^{133}Sn decays (and also the decay to the ^{133}Sb $\frac{7}{2}^-$ ground state), ^{134}Sn$(0^+) \rightarrow$ ^{134}Sb(1_1^-), and ^{134}Sb$(0^-) \rightarrow$ ^{134}Te$(2_{1,2}^+, 1_1^+)$. For this group the predictions are in excellent agreement with experiment. The second group is composed of ^{134}Sn(0^+) $\rightarrow$ ^{134}Sb(1_2^-), ^{134}Sb$(0^-) \rightarrow$ ^{134}Te(2_3^+), and ^{134}Sb$(7^-) \rightarrow$ ^{134}Te$(6_{1,2}^+)$. For this group the overall agreement with experiment is poor. (As discussed in Sec. IV C, we view

TABLE V. Comparison of predicted and experimental values of $\langle C(W)\rangle^{1/2}$ for the $A = 133$-134 β^- branches under consideration.

Transition		E_x (keV)			$\langle C(W)\rangle^{1/2}$ (fm)				
Initial	Final	Expt.	KH	CW	Expt.	KH		CW	
						H7B	HBB	H7B	HBB
^{133}Sn$(\frac{7}{2}^-)$	^{133}Sb$(\frac{5}{2}^+)$	962	962	920	30.1±3.4	37.3	40.0	37.3	40.0
^{133}Sn$(\frac{7}{2}^-)$	^{133}Sb$(\frac{3}{2}^+)$	2708	2708	2641	5.5±0.8	2.4	3.4	2.4	3.4
^{134}Sn(0^+)	^{134}Sb(1^-)	318	0	318	12.1±3.3	13.2	13.6	18.3	18.9
^{134}Sn(0^+)	^{134}Sb(1^-)	872	695	872	35.0±7.7	59.3	63.1	58.9	62.4
^{134}Sb(0^-)	^{134}Te(2^+)	1279	1182	1330	<7.8	5.0	5.1	6.2	6.3
^{134}Sb(0^-)	^{134}Te(2^+)	2464	2366	2485	7.3±2.0	6.8	7.6	6.5	7.0
^{134}Sb(0^-)	^{134}Te(1^+)	2632	2291	2650	24.7±2.3	30.3	30.9	28.0	30.5
^{134}Sb(0^-)	^{134}Te(2^+)	2934	2981	3134	10.8±4.6	0.1	0.2	0.1	0.3
^{134}Sb(7^-)	^{134}Te(6^+)	1691	1468	1703	21.4±1.3	5.3	5.7	5.2	5.5
^{134}Sb(7^-)	^{134}Te(6^+)	2398	2134	2293	31.4±1.9	30.9	33.0	30.9	33.0

TABLE VI. Intensities of ($\nu Q' = 5$) and ($\pi Q' = 4$) pairs in the CW4082 ^{134}Sn and ^{134}Te ground states, respectively.

^{134}Sn		^{134}Te	
Orbit	Intensity (%)	Orbit	Intensity (%)
$1f_{7/2}$	51.0	$0g_{7/2}$	80.3
$2p_{3/2}$	7.7	$1d_{5/2}$	12.7
$2p_{1/2}$	3.0	$1d_{3/2}$	2.4
$0h_{9/2}$	14.6	$2s_{1/2}$	1.0
$1f_{5/2}$	10.1	$0h_{11/2}$	3.4
$0i_{13/2}$	10.0		

the agreement for decay to the 6_2^+ level of ^{134}Te as fortuitous.) The results for the decay of ^{134}Sn also depend on its ground-state wave function shown together with that for the ^{134}Sb ground state in Table VI. The other initial states are quite pure, i.e., the ^{133}Sn ground is a single-particle state and, as shown in Table III, the 0_1^- and 7_1^- states of ^{134}Sb have quite pure $\nu 1f_{7/2}\pi 0g_{7/2}$ wave functions.

A. Decay of ^{133}Sn($\frac{7}{2}^-$)

These are conceptually the simplest decays being considered since, as shown in Fig. 6, they are single-particle transitions in first order. Contrary to expectations, the role of the initial state admixtures of the $\pi 0g_{9/2}$ orbit was found to be of minor importance. The quenching due to this orbit of M_1^u in the decay to the $\frac{5}{2}^+$ state and of M_2^z in the decay to the $\frac{3}{2}^+$ state were 7.6% and 3.3%, respectively. These results are typical of the others under consideration. In contrast, the final-state correlations have large effects as can be seen from Table IV. Note that the predicted (HBB) q_α value of 0.17 for the $R2$ decay to the $\frac{3}{2}^+$ state means a decrease in the decay rate by a factor of 36. (This value appears to be overestimated, with $q_\alpha \sim 14$ indicated by experiment. The difficulty with this particular q_α was discussed in Sec. III.) Clearly an accurate determination of these core polarization effects is paramount. The $R1$ and $R2$ contributions to the decay of ^{133}Sn($\frac{7}{2}^-$) to the $\frac{7}{2}^+$ ground state of ^{133}Sb was also considered. We predict that these contribute 1.4% to this branch, i.e., the branch is 98.6% rank-zero ($R0$).

B. Decay of ^{134}Sb(7^-)

We consider this decay next because it exemplifies most simply the problem with the second group of final state discussed above, i.e., those with mixed wave functions. Other than the known branches to the first two 6^+ states listed in Tables I and V, our results indicate no first-forbidden branches (including $R0$ decays to 7^+ states) >0.01% other than 0.84% and 0.21% for the first two 5^+ states, which are predicted to lie at excitation energies of 2791 and 4635 keV, respectively. The predictions of Table V for the 6_1^+ state are seen to disagree greatly with experiment. Possible reasons for this disagreement were explored and the most likely source was found to lie in the $J = 6$ proton-proton off-diagonal matrix element $\langle 0g_{7/2}0g_{7/2}|V|0g_{7/2}1d_{5/2}\rangle$ which is responsible for the mixing between the two lowest 6^+ states. The problem can be understood by reference to Table VII which shows the contributions of the orbits to the sum of Eq. (1) for the two $R1$ matrix elements. Because they combine destructively, the final values of $\langle C(W)\rangle^{1/2}$ are sensitive to the balance between M_1^u and M_1^x. For both states M_1^x gives the larger contribution to $B_1^{(1)}$ but the cancellation between M_1^u and M_1^x is much more complete for the 1691-keV level. The two states are essentially

TABLE VII. CW4082 predictions for the $R1$ $D_R(j_i j_f)$ and matrix elements of Eq. (1) for the decay of ^{134}Sb(7^-) to the 1691 and 2398 keV 6^+ states of ^{134}Te.

νj_i	πj_f	$D_1(j_i j_f)$	$M_1^u(j_i j_f, \text{eff})$	$\mathcal{M}_1^u(j_i j_f)$	$M_1^x(j_i j_f, \text{eff})$	$\mathcal{M}_1^x(j_i j_f)$
			The 6_1^+ 1691-keV level			
$0h_{9/2}$	$0g_{9/2}$	0.0343	−3.2767	−0.1125	0.2625	0.0090
$1f_{7/2}$	$0g_{9/2}$	0.0130	−0.7901	−0.0103	0.7571	0.0098
$0h_{9/2}$	$0g_{7/2}$	−0.0858	−1.4377	0.1234	1.9173	−0.1645
$1f_{7/2}$	$0g_{7/2}$	−0.6133	−1.0536	0.6462	−0.1875	0.1150
$1f_{5/2}$	$0g_{7/2}$	0.0003	1.0206	0.0003	0.8661	0.0003
$1f_{7/2}$	$1d_{5/2}$	0.3897	1.4567	0.5676	1.6791	0.6543
		Total:		1.2147		0.6237
			The 6_2^+ 2398-keV level			
$0h_{9/2}$	$0g_{9/2}$	−0.0558	−3.2767	0.1828	0.2625	−0.0147
$1f_{7/2}$	$0g_{9/2}$	0.0347	−0.7901	−0.0274	0.7571	0.0263
$0h_{9/2}$	$0g_{7/2}$	0.0695	−1.4377	−0.0999	1.9173	0.1332
$1f_{7/2}$	$0g_{7/2}$	−0.1844	−1.0536	0.1943	−0.1875	0.0346
$1f_{5/2}$	$0g_{7/2}$	0.0002	1.0206	0.0002	0.8661	0.0002
$1f_{7/2}$	$1d_{5/2}$	−1.2995	1.4567	−1.8929	1.6791	−2.1820
		Total:		−1.6421		−2.0010

orthogonal mixtures of $(0g_{7/2})^2$ and $0g_{7/2}1d_{5/2}$ with the percentage of these two terms in the 1691-keV level being 92 and 8, respectively. Two noteworthy features of these decays are the very small value of $M_1^x(1f_{7/2}0g_{7/2},\text{eff})$ (so that the 8% $1f_{7/2}1d_{5/2}$ in the 1691-keV wave function is quite important) and the fact that for the 1691-keV level $\mathcal{M}_1^u(1f_{7/2}0g_{7/2})$ and $\mathcal{M}_1^u(1f_{7/2}1d_{5/2})$ are closely equal in magnitude and add in phase. After consideration of all possibilities, it seems that the only way to obtain values of $\langle C(W)\rangle^{1/2}$ close to the experimental ones within our model space is to change the relative phases of $\mathcal{M}_1^u(1f_{7/2}0g_{7/2})$ and $\mathcal{M}_1^u(1f_{7/2}1d_{5/2})$. This is done by changing the sign of the $J=6$ $\langle 0g_{7/2}0g_{7/2}|V|0g_{7/2}1d_{5/2}\rangle$ TBME. For instance, with this TBME changed from +0.169 to −0.250 MeV the $\langle C(W)\rangle^{1/2}$ become 20.1 and 28.5 fm, respectively, while the percentages of $(0g_{7/2})^2$ and $0g_{7/2}1d_{5/2}$ in the 6_1^+ state become 85 and 15, respectively.

C. Decay of ^{134}Sb(0^-)

Aside from the known branches listed in Table I, we predict no other first-forbidden branch (including $R0$ decays) greater than 0.5%. The results are in excellent accord with experiment with the exception of the decay to the third 2^+ state. The experimental branch to this state has a large uncertainty and the J^π value is uncertain so that the disagreement may not be real. If it is real then the likely problem would be that the mixing between the 2_3^+ and 2_4^+ states is not given correctly by the interactions. This would not be surprising since these two states are rather closely orthogonal mixtures of $0g_{7/2}1d_{3/2}$ and $(1d_{5/2})^2$ while, in contrast, the 2_1^+ and 2_2^+ states are quite pure $(0g_{7/2})^2$ (90%) and $(1d_{5/2})^2$ (92%), respectively. The 1_1^+ state of ^{134}Te is 98.5% $0g_{7/2}1d_{5/2}$ for the CW4082 interaction. Thus the transition to it from the ^{134}Sb 0^- ground state—which is 95.5% $\nu 1f_{7/2}\pi 0g_{7/2}$—is a rather pure $\nu 1f_{7/2}\rightarrow\pi 1d_{5/2}$ transition. The excellent agreement with experiment is a successfully passed test of the core polarization.

D. Decay of ^{134}Sn(0^+)

In addition to the $R1$ branches to the first two 1^- states of ^{134}Sb, significant first-forbidden branches are predicted for other bound 1^- and 2^- states of ^{134}Sb. These predictions are collected in Table VIII. The ^{134}Sb 1_1^- state is quite pure $\nu 1f_{7/2}\pi 0g_{7/2}$ and agreement with experiment for the decay to it is excellent. The 1_2^- and 1_3^- ^{134}Sb states have mixed wave functions with each other and other states as well (see Table III). The situation is more complex than for the 6^+ states of ^{134}Te discussed above. Agreement with experiment for the branch to the 1_2^- state could be achieved with minor changes in off-diagonal matrix elements.

In addition to the three known decays to bound states of ^{134}Sb, ^{134}Sn decays with a branch of 13±7 % to a state at 3850 keV. The $\log f_0 t$ value for this decay is 4.41 ± 0.29 from which the 3850-keV level is assigned $J^\pi = 1^+$ [1]. Using

$$B(\text{GT}) = 6166/f_0 t, \tag{4.1}$$

we find a B(GT) value of 0.24 ± 0.16 for the branch to the 1_1^+ state which is 100% $\nu 0h_{9/2}\pi 0h_{11/2}$ in the two 5082 model spaces. The predicted value of B(GT) for both the KH4082 and CW4082 interactions is B(GT) = 1.06 with no quenching. The quenching of the Gamow-Teller strength in nuclear matter is known to be ≈0.6 which results in a predicted B(GT) about twice the experimental value. Note that for our model space this transition results entirely from a $\nu 0h_{9/2}\rightarrow\pi 0h_{11/2}$ transition and thus the B(GT) is directly proportional to the percentage of $(\nu 0h_{9/2})^2$ in the ^{134}Sn ground state.

TABLE VIII. $\langle C(W)\rangle^{1/2}$ values and branching ratios (B) predicted with the CW4082 and HBB interactions for ^{134}Sn(0^+) decay to bound 1^- and 2^- states of ^{134}Sb. The excitation energies are those of the CW5082 interaction.

J^π	E_x (keV)	$\langle C(W)\rangle^{1/2}$ (fm)	B (%)
1^-	318	18.8	3.4
2^-	376	3.0	0.09
1^-	872	62.4	25.5
2^-	881	11.7	0.89
2^-	1234	10.3	0.69
1^-	1740	24.6	2.3
2^-	1780	2.5	0.02
1^-	1947	17.8	1.0
1^-	2062	8.3	0.18
2^-	2085	1.1	0.00
2^-	2226	0.6	0.00
2^-	2431	1.1	0.00
1^-	2622	18.5	0.59
2^-	2668	0.3	0.00
2^-	2811	0.1	0.00

V. SUMMARY

A general conclusion from the discussion of β^- decay given in the preceding section is that the core polarization is essentially correct but the residual interactions do not give the detailed mixing of states very well. A specific failure of the CW4082 interaction (the KH4082 interaction has the same failing) was detailed for the ^{134}Sb(7^-) $\rightarrow$ ^{134}Te($6_{1,2}^+$) decays. Similar but smaller changes would give better agreement for the ^{134}Sn $\rightarrow$ ^{134}Sb(1_2^-) decay.

It was emphasized that an unusual uncertainty in our residual interactions was in the placement of the neutron single-particle energies. How severely do the β^- decay results test this placement? The answer is not very severely at all. Granted that the 0_1^- and 7_1^- states of ^{134}Sb are nearly pure $\nu 1f_{7/2}\pi 0g_{7/2}$ (see Table III) the only significant dependence on these single-particle energies is via

the ^{134}Sn groundstate wave function (Table VI) and the wave function of the 1_2^- state of ^{134}Sn.

We emphasized in the Introduction that the main motive for this work was to build and test residual interactions to apply to the $R0$ $\Delta J = 0$ decays of Table I. From the results given here it can be inferred that the interactions are quite adequate for this purpose since the $R0$ decays involve states which are akin to the group of states for which good agreement was achieved for the $R1$ and $R2$ decays.

ACKNOWLEDGMENTS

We would like to thank Guy Walter for calling these decays to our attention, B. Fogelberg for communication of experimental results prior to publication, and A. Hosaka for communicating (via B. A. Brown) his results for the HBB potential. B. A. Brown and D. J. Millener provided valuable counsel. Research was supported by the U.S. Department of Energy under Contract No. DE-AC02-76CH00016.

[1] B. Fogelberg, B. Ekström, L. Sihver, and G. Rudstam, Phys. Rev. C **41**, R1890 (1990); B. Fogelberg, private communication.
[2] E. K. Warburton, Phys. Rev. C **44**, 233 (1991).
[3] E. K. Warburton, Phys. Rev. C **42**, 2479 (1990).
[4] Y. V. Sergeenkov and V. M. Sigalov, Nucl. Data Sheets **49**, 639 (1986). $A = 133$.
[5] Y. V. Sergeenkov and V. M. Sigalov, Nucl. Data Sheets **34**, 475 (1986). $A = 134$.
[6] L. Spanier, B. Fogelberg, and M. Hellstrom, private communication from B. Fogelberg.
[7] G. Rudstam, K. Aleklett, and L. Sihver, private communication from B. Fogelberg.
[8] J. Blomqvist, A. Kerek, and B. Fogelberg, Z. Phys. A **314**, 199 (1983).
[9] A. H. Wapstra and G. Audi, Nucl. Phys. **A432**, 1 (1985); midstream update, P. E. Haustein, private communication (1990).
[10] T. T. S. Kuo and G. Herling, U.S. Naval Research Laboratory Report No. 2258, 1971 (unpublished).
[11] J. B. McGrory, Phys. Rev. C **8**, 693 (1973).
[12] E. K. Warburton and B. A. Brown, Phys. Rev. C **43**, 602 (1991).
[13] The discovery of ^{133}In and a preliminary report on its decay was reported by J. Blomqvist *et al.* in a private communication cited in Ref. [1].
[14] H. G. Kruse and B. H. Wildenthal, Bull. Am. Phys. Soc. **27**, 533 (1982).
[15] J. E. Park, W. W. Daehnick, and M. J. Spisak, Phys. Rev. C **15**, 587 (1977).
[16] L. K. Peker, Nucl. Data Sheets **45** 1 (1985). $A = 141$.
[17] A. Hosaka, K.-I. Kubo, and H. Toki, Nucl. Phys. **A244**, 76 (1985).
[18] B. A. Brown, A. Etchegoyen, W. D. M. Rae, and N. S. Godwin, computer code OXBASH, 1984 (unpublished).
[19] M. Lacombe, B. Loiseau, J. M. Richard, R. Vinh Mau, J. Côté, P.Pirès, and R. de Tourreil, Phys. Rev. C **21**, 861 (1980).
[20] A. Hosaka, private communication to B. A. Brown.
[21] R. Machleidt, K. Holinde, and C. Elster, Phys. Rep. **149**, 1 (1987).
[22] G. E. Brown and M. Rho, Phys. Lett. B **327**, 283 (1990).
[23] E. K. Warburton, Phys. Rev. C **45**, 463 (1992).